Original article

MOLECULAR METABOLISM

Limited OXPHOS capacity in white adipocytes is a hallmark of obesity in laboratory mice irrespective of the glucose tolerance status

Theresa Schöttl, Lisa Kappler, Tobias Fromme, Martin Klingenspor*

ABSTRACT

Objective: Several human and rodent obesity studies speculate on a causal link between altered white adipocyte mitochondria in the obese state and changes in glucose homeostasis. We here aimed to dissect whether alterations in white adipocyte mitochondrial respiratory function are a specific phenomenon of obesity or impaired glucose tolerance or both.

Methods: Mature white adipocytes were purified from posterior subcutaneous and intraabdominal epididymal fat of four murine obesity models characterized by either impaired or normal oral glucose tolerance. Bioenergetic profiles, including basal, leak, and maximal respiration, were generated using high-resolution respirometry. Cell respiratory control ratios were calculated to evaluate mitochondrial respiratory function.

Results: Maximal respiration capacity and cell respiratory control ratios were diminished in white adipocytes of each of the four murine obesity models, both in the absence and the presence of impaired glucose tolerance. Limitation was more pronounced in adipocytes of intraabdominal versus subcutaneous fat.

Conclusion: Reduced mitochondrial respiratory capacity in white adipocytes is a hallmark of murine obesity irrespective of the glucose tolerance status. Impaired respiratory capacity in white adipocytes solely is not sufficient for the development of systemic glucose intolerance.

Keywords Obesity; Glucose tolerance; White adipocyte metabolism; Mitochondria

1. INTRODUCTION

Mass-specific resting metabolic rate of white adipose tissue (WAT) is low and may appear negligible compared to the high metabolic rate of organs such as brain, kidneys, heart or liver [1,2]. Statistical modeling of whole body energy expenditure, however, reveals an unexpectedly large contribution of adipose tissue mass to the intra-individual variation in resting metabolic rate. This is not caused by the metabolic cost of the adipose organ itself but rather by the influence on metabolism of other organs including liver and skeletal muscle, most likely involving the well-established endocrine function of adipocytes in body energy and glucose homeostasis regulation [3]. Thus, the impact of adipocyte function on whole body energy and glucose metabolism is much larger than expected from their intrinsic metabolic rate.

Mitochondria are the major site of energy turnover in cells consuming oxygen for ATP synthesis by oxidative phosphorylation (OXPHOS). Furthermore, they play a central role in the metabolism of reactive oxygen species (ROS), the regulation of apoptosis and the regulation of calcium levels in both cytoplasm and matrix, in addition to many other functions [4,5]. In adipocytes, proper mitochondrial function is essential for differentiation, lipogenesis and lipolysis [6], as well as the production and secretion of adipokines [7]. Thus, alterations in white adipocyte mitochondrial function can be expected to affect adipocyte physiology with tremendous secondary effects on whole body energy and glucose homeostasis.

Several human and rodent studies highlighted the simultaneous appearance of deranged white adipocyte mitochondria and impaired glucose homeostasis. Mitochondrial biogenesis and abundance, the expression of genes and proteins involved in OXPHOS, and mitochondrial oxygen consumption, as a key parameter for mitochondrial function, are reduced in WAT or isolated adipocytes of obese and/or type 2 diabetic rodent models and humans [8–13]. Moreover, we recently uncovered reduced mitochondrial OXPHOS functionality in white adipocytes, which emerges in parallel with impaired glucose tolerance after one week of high-fat diet feeding [14]. The fact that obesity is often accompanied by impaired glucose tolerance and reduced adipocyte mitochondrial function, however, does not prove causality between these phenomena. The ultimate challenge is to clarify the relationship between obesity, white adipocyte mitochondrial function, and glucose intolerance.

In the present study, we determined glucose tolerance and white adipocyte OXPHOS, as a parameter for mitochondrial function, in anatomically distinct fat depots of several murine obesity models. We first comprehensively analyzed mitochondrial respiration of isolated adipocytes from both posterior subcutaneous and intraabdominal epididymal fat of diet-induced obese mice with pronounced glucose

Molecular Nutritional Medicine, Technische Universität München, Else Kröner Fresenius Center for Nutritional Medicine, Freising, Germany

*Corresponding author. Molecular Nutritional Medicine, Technische Universität München, Gregor-Mendel-Str. 2, D-85356 Freising-Weihenstephan, Germany. Tel.: +49 8161 71 2386; fax: +49 8161 71 2366. E-mail: mk@tum.de (M. Klingenspor).

Received June 16, 2015 • Revision received July 3, 2015 • Accepted July 7, 2015 • Available online 15 July 2015

http://dx.doi.org/10.1016/j.molmet.2015.07.001

Abbreviations

AUC	area under the curve
BSA	bovine serum albumin
CD	control diet
cRCR	cell respiratory control ratio
CS	citrate synthase
ETC	electron transport chain
eWAT	epididymal white adipose tissue
HFD	high-fat diet
psWAT	posterior subcutaneous white adipose tissue
Mc4R	melanocortin-4-receptor
OXPHOS	oxidative phosphorylation
RCR	respiratory control ratio
ROS	reactive oxygen species
T2DM	type 2 diabetes mellitus
WAT	white adipose tissue

intolerance, describing the extent of functional mitochondrial alterations associated with obesity and/or glucose intolerance. Second, we demonstrated mitochondrial OXPHOS capacity to be limited in any state of elevated body fat content by experimenting with diet-induced obese mice with recovered glucose tolerance in response to energy restriction and two monogenetic models of obesity.

2. MATERIALS AND METHODS

2.1. Mice

All experiments were conducted on male mice. Before and throughout the whole experiment, mice were housed in groups in a specific pathogen-free environment on a 12:12 h light–dark photocycle at 22 °C with ad libitum access to water and food.

The study was performed with permission of the government of Upper Bavaria (Regierung von Oberbayern, reference number Az. 55.2.1.54-2532-148-13).

2.1.1. Diet induced obesity models

At the age of 7 weeks, wildtype C57BL/6N mice were switched from chow (type M-Z, Ssniff, Soest, Germany) to a purified research control diet (CD, 12 kJ% fat, SS745-E702, Ssniff). After an acclimatization phase of one week, mice were matched by body weight into a CD and a high-fat diet group (HFD, 48% kJ% fat SS745-E712; Ssniff). Feeding was conducted for 24 weeks. Mice of the HF-recovery cohort received CD for one week subsequent to HFD feeding for 24 weeks. Mice were killed and dissected at the end of the respective feeding period.

2.1.2. Genetic obesity

$Lep^{ob/ob}$ mice and mice with melanocortin-4-receptor (Mc4R) deficiency, including $Mc4R^{X16/X16}$, are well established models for monogenetic obesity characterized by enormous weight and fat mass gain on a regular diet [15,16].

$Mc4r^{X16/X16}$ – Generation of $Mc4r^{X16/X16}$ knock-in mice has been described in detail before [16]. At the age of 7 weeks $Mc4r^{X16/X16}$ mice and $Mc4r^{wt/wt}$ littermates were switched from normal chow to CD diet until dissection at the age of 32 weeks.

$Lep^{ob/ob}$ – $Lep^{ob/ob}$ mice and wildtype $Lep^{+/+}$ littermates received normal chow diet until dissection at the age of 14 weeks.

2.1.3. Body weight and body composition

Body weight and body composition (analyzed with nuclear magnetic resonance spectroscopy -The Minispec mq 7.5 POY Live mice analyzer, Bruker, Billerica, MA, USA) of all mice were measured at the end of experimental duration (HFD versus CD: after 24 weeks feeding, $Mc4R^{X16/X16}$ versus $Mc4R^{wt/wt}$: at the age of 32 weeks, $Lep^{ob/ob}$ versus $Lep^{+/+}$: at the age of 14 weeks, HF-recovery mice and controls: after 24 weeks HFD/CD feeding when HFD was replaced by CD as well as after one week CD refeeding).

2.1.4. Oral glucose tolerance

After a fasting period of six hours, mice received 2.66 mg glucose per [(lean mass + 0.2 fat mass) g] by single oral gavage, referring to [17]. Blood glucose was monitored before and 15, 30, 60 and 90 min after gavage. Total area-under-the-curve (AUC) was calculated as measure for glucose tolerance.

2.1.5. Plasma insulin levels

For plasma preparation, cardiac blood was sampled from CO_2 anesthetized mice in heparin-coated tubes and centrifuged for 2 min at 2000 *g*. Plasma concentration of insulin was ascertained using a commercial Kit system (Ultra Sensitive Mouse Insulin ELISA Kit, 90080 Christyl Chem, Downers Grove, IL, USA).

2.2. Tissue dissection and isolation of adipocytes

Mice were killed by carbon dioxide exposure and exsanguination. Posterior subcutaneous and intraabdominal epididymal fat depots were dissected and weighed. For assessment of adipocyte bioenergetics on the cellular level, fat depots of individual mice were used. Due to the low yield of mitochondria per ml adipocyte suspension at mitochondrial isolation, fat depots of 8–12 mice were combined for experiments on isolated mitochondria. Therefore, fat pools were generated for posterior subcutaneous and intraabdominal epididymal fat separately, and they were analyzed individually throughout our study. Mature adipocytes were separated from other cell types by collagenase-digestion as described in detail previously [14] (collagenase type A, Roche Applied Science; Penzberg, Germany; 1 g/l in Hank's Balanced Salt Solution [HBSS 14025-092, Gibco®, life technologies, Carlsbad, CA, USA] containing 4% BSA). Isolated mature adipocytes were washed with STE-buffer containing 4% BSA-fatty acid free (250 mM sucrose, 5 mM Tris, 2 mM EGTA, pH = 7.4 at 4 °C).

2.3. Characterization of isolated mature adipocytes

2.3.1. Bioenergetics

Oxygen consumption of adipocytes was measured with high-resolution respirometry (Oxygraph-2k, OROBOROS INSTRUMENTS, Innsbruck, Austria) as described previously [14]. Briefly, 100 µl of adipocyte suspension was pipetted into 2 ml MIR05 buffer (110 mM sucrose, 60 mM potassium lactobionate, 0.5 mM EGTA, 3 mM $MgCl_2$*$6H_2O$, 20 mM taurine, 10 mM KH_2PO_4, 20 mM Hepes, 1 g/l BSA-fatty acid free, 5 mM malate, pH 7.1 at 37 °C, as described by OROBOROS INSTRUMENTS). First, pyruvate (5 mM) was added, and basal cellular respiration was recorded. Respiration determined by proton leak was assessed by addition of complex V inhibitor oligomycin (2.5 µg/ml). Titration of FCCP (0.5 µM steps) was performed to measure maximal cellular respiration rates. Non-mitochondrial oxygen consumption was determined by addition of complex III inhibitor antimycin A (2.5 µM) and subtracted from the other respiratory states. Spare respiratory capacity was calculated by subtracting basal from maximal oxygen consumption. For mitochondrial integrity control cell respiratory control

ratio (cRCR) was calculated as ratio of maximal to leak oxygen consumption.

2.3.2. Cellular DNA quantification

DNA content of adipocyte suspensions was assessed by quantitative PCR targeting a unique region of genomic DNA (promotor resistin) as described previously (primers: fw 5′-ACCTCTCTTGGGGTCAGATGT-3′, rev 5′-CTGGGTATTAGCTCCTGTCCC-3′) [14].

2.3.3. Citrate synthase activity

Citrate synthase activity was measured as a surrogate for mitochondrial content in adipocyte suspensions. Adipocyte suspensions were homogenized and diluted 1:25 in reaction buffer (100 mM Tris, 1 mM $MgCl_2$, 1 mM EGTA, 0.1 mM DTNB, 3.6 mM Acetyl-CoA, pH 8.2). Absorption was measured at 30 °C and 412 nm with a microplate reader (TECAN Infinite® M200, Tecan Group Ltd.; Männedorf, Switzerland) before and after oxaloacetate (0.5 mM) was injected. Enzyme activity [μmol/min*mg protein] was calculated on the basis of the absorption change before and after injection of oxaloacetate with respect to dilution factor, extinction coefficient of DTNB and path length of the plate.

2.4. Characterization of isolated mitochondria

2.4.1. Isolation of mitochondria

Mitochondrial isolation from adipocytes was performed as already described [14]. Briefly, mature adipocytes were transferred into a glass-teflon homogenizer (15 ml), filled with STE to 15 ml and disrupted by 5 rotating strokes. Mitochondria were isolated from the homogenate via differential centrifugation (10 min at 800 *g*, 10 min at 10,000 *g*). Pellets were resuspended in KHE-buffer (120 mM KCL, 5 mM KH_2PO_4, 3 mM HEPES, 1 mM EGTA, 0.5% BSA-fatty acid free, pH = 7.2). Protein concentration determination of mitochondrial suspensions by Bradford protein assay was performed as described previously [14].

2.4.2. Bioenergetics

Oxygen consumption of isolated mitochondria was measured using microplate respirometry (XF96 Extracellular Flux Analyzer, Seahorse Bioscience, Billerica, MA, USA). Isolated mitochondria diluted in 20 μl KHE-buffer were seeded in collagen coated XF96-PS cell culture plates (Seahorse Bioscience, 5 μg per well). Mitochondrial respiration was measured in the presence of substrate only (complex I linked substrates: pyruvate and palmitoyl-L-carnitine; complex II substrate: succinate, state 4). ADP (6 mM) was injected to induce phosphorylating respiration (state 3). Next, 2.5 μg/ml oligomycin was injected to inhibit ATP-synthase and measure leak respiration (state 4o). The chemical uncoupler carbonyl cyanide 4-(trifluoromethoxy) phenylhydrazone FCCP (4 μM) was added for measuring maximal uncoupled respiration rates (state 3u). Finally, non-OXPHOS oxygen consumption was assessed by the addition of antimycin A (4 μM) and rotenone (2 μM) and subtracted from values of the other conditions. Terminology of respiratory states refers to [4]. Oxygen consumption was calculated automatically by plotting oxygen concentration (nmoles O_2) versus time (min), using the original (gain) fixed algorithm of the XF Software. Respiratory control ratios were ascertained by dividing oxygen consumption during state 3 respiration by oxygen consumption during state 4o respiration.

2.4.3. Measurement of mitochondrial ROS

Mitochondrial H_2O_2 efflux was assessed using Amplex® Red fluorescence. Measurements and analysis were performed as described before [14]. Substrates: 5 mM pyruvate/5 mM malate, 40 μM palmitoyl-L-carnitine, 5 mM malate.

2.5. Immunoblotting

Mitochondrial protein (25 μg) was resolved on a 7.5% SDS-PAGE, transferred to a nitrocellulose membrane (LI-COR Bioscienes, Lincoln, NE, USA; 60 min, 100 V) and probed with an antibody cocktail targeting one representative subunit of each of the five ETC complexes (MitoProfile® total OXPHOS Rodent WB Antibody Cocktail, 1:250, ab110413, complex I subunit NDUFB8, complex II-30kDa, complex III-Core protein 2, complex IV subunit I, complex V alpha subunit) and rabbit anti-protein voltage-dependent anion channel (VDAC) antibody (1:900, Calbiochem, PC548). Infrared dye conjugated secondary antibodies (IRDye® 680, IRDye® 800, LI-COR Biosciences) were incubated at a dilution of 1:20,000. The Odyssey software (LI-COR Biosciences) was applied to quantify band fluorescence intensities.

2.6. Statistical analyses

Data are presented as single or mean values ± standard deviation. For statistical comparison, Two-Way and Two-Way Repeated-Measures ANOVA followed by post-hoc Bonferroni testing, One-Way ANOVA followed by Tukey's multicomparison test or two-tailed Student's t-test were performed (SigmaPlot 12.5, Systat Software, Inc., San Jose, CA, USA; GraphPad Prism4, GraphPad Software, Inc., La Jolla, CA, USA). p Values < 0.05 were considered statistically significant.

3. RESULTS

3.1. Diet induced obesity is associated with glucose intolerance and limited mitochondrial OXPHOS capacity in white adipocytes

We analyzed the impact of obesity on glucose tolerance and white adipocyte mitochondrial oxidative phosphorylation (OXPHOS) with special attention to a) a possible association between both phenomena and b) differences in anatomically distinct fat depots.

As a first step, we determined glucose tolerance and white adipocyte mitochondrial OXPHOS functionality in subcutaneous and intra-abdominal fat of diet-induced obese mice. At the end of a 24 weeks feeding period, high-fat diet (HFD) fed mice were massively obese as indicated by a higher body and fat mass at a comparable lean mass (Figure 1A–C). Posterior subcutaneous and intraabdominal epididymal fat depots were significantly larger in HFD vs. CD fed mice, reflecting their contribution to whole body adiposity (posterior subcutaneous: HFD 2.836 g ± 0.636 g vs. CD 0.704 g ± 0.255 g; epididymal: HFD 1.714 g ± 0.441 g vs. CD 0.710 g ± 0.311 g, both $n = 38–41$, $p < 0.001$). Diet-induced obesity was accompanied by hyperinsulinemia and impaired oral glucose tolerance, reflected by lower glucose clearance and higher area under the curve (AUC, Table 1, Figure 1D,E).

We prepared mitochondria from adipocytes of both fat depots to study organelle respiratory function free of other cellular influences and undisturbed by differences in mitochondrial abundance [4]. Leak respiration (substrate only = state 4, and state 4o) of mitochondria from both fat depots of the HFD group tended to be lower irrespective of the substrate applied (succinate, pyruvate or palmitate), but this diet effect did not reach significance. In contrast, mitochondria from the HFD group consistently stood out by a marked reduction of phosphorylating (state 3) and maximal respiratory capacity (state 3u) (Figure 2A).

Respiratory control ratio (RCR, state 3/state4o) is a quality index for mitochondrial respiratory function reflecting the ability to generally run at idle but efficiently respond to ADP supply by high ATP production

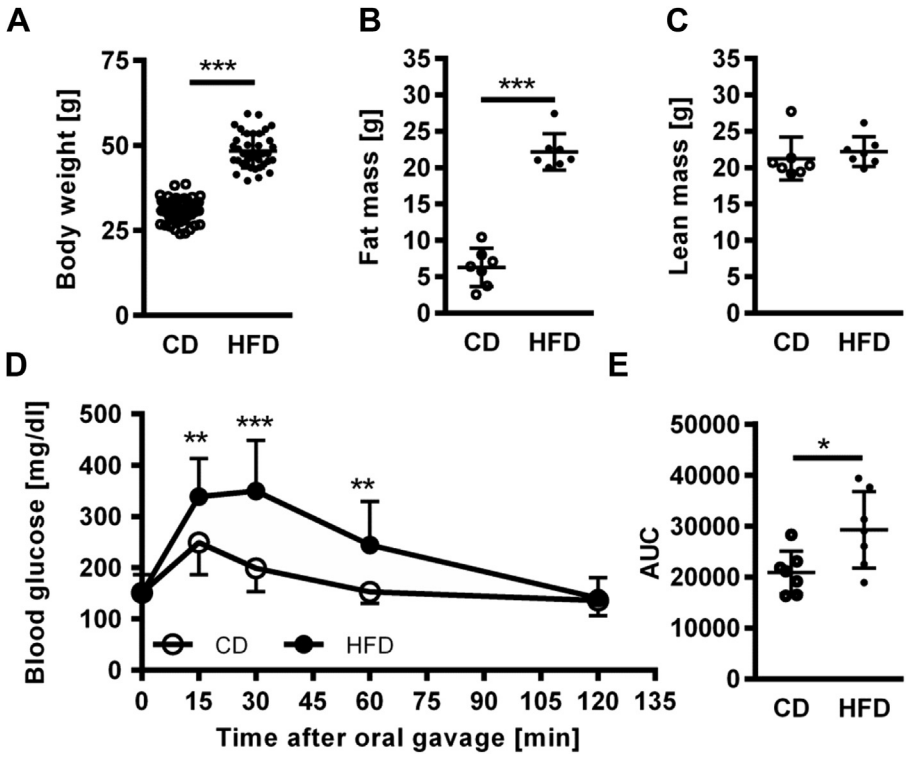

Figure 1: 24 weeks HFD feeding causes massive obesity and impaired glucose tolerance. At the age of eight weeks, mice were matched by body weight into HFD and CD groups. Diets were fed for 24 weeks. All parameters were measured at the end of the feeding period. (A) Body weight (n = 38–41), (B) Fat mass (n = 7), (C) Lean mass (n = 7), (D) Oral glucose tolerance test (n = 7), (E) Total area-under-the-curve (AUC) calculated from D as measure for glucose tolerance (n = 7). A, B, C, E was analyzed by Student's t-test. D was analyzed by two way repeated measures ANOVA. Data are presented as means ± SD. * = $p < 0.05$, ** = $p < 0.01$, *** = $p < 0.001$.

rates [4]. For mitochondria respiring on pyruvate or palmitate, but not succinate, we observed decreased RCRs in the HFD group (Figure 2B). Thus, HFD induced obesity caused a limitation in white adipocyte mitochondrial OXPHOS in posterior subcutaneous and epididymal adipocytes in states when maximal substrate oxidation capacity limits respiration (state 3, state 3u). Notably, the degree of impairment depended on the entry point of electrons into the respiratory chain: deficits were more pronounced in mitochondria respiring on complex I vs. complex II substrates, indicated by lower RCRs for pyruvate and palmitate but not succinate.

Lower abundance of respiratory chain complexes has been associated with lower OXPHOS capacity in mitochondria [18]. Thus, we quantified protein amount of representative subunits of each of the five OXPHOS complexes in relation to a surrogate marker of total mitochondrial abundance, the outer membrane channel porin/VDAC. Diet-group comparison revealed a significant reduction of the five enzyme complexes in both posterior subcutaneous ($p < 0.001$) and epididymal adipocyte mitochondria ($p < 0.01$) of HFD fed mice (Figure 3). Together, the lower absolute respiration capacity of isolated white adipocyte mitochondria of the HFD group may be explained by a decreased abundance in electron transport chain complexes per mitochondrion.

Elevated levels of reactive oxygen species (ROS) in adipocytes have been associated with obesity dependent impaired glucose tolerance and insulin resistance [19]. We determined whether mitochondria from posterior subcutaneous and epididymal adipocytes of HFD vs. control diet (CD) fed mice differ in terms of H_2O_2 efflux, as a result of superoxide radical anion formation. Superoxide, the main ROS produced by the electron transport chain, is converted by superoxide dismutase 2 (SOD2) to membrane permeable H_2O_2 [20,21] which is either

Table 1 — Plasma levels of insulin (non-fasted) and glucose (fasted and non-fasted) of different mouse models of obesity.

	Insulin [ng/ml]	Glucose [mg/dl] fasted	Glucose [mg/dl] non-fasted	n
CD	1.32 ± 0.93	150.90 ± 17.53	156.10 ± 14.93	5–7
HFD	11.66 ± 3.71***, a	149.20 ± 39.94	163.00 ± 38.47	6–7
CD (recovery model)	1.53 ± 0.63	140.70 ± 12.34	157.40 ± 12.90	6–7
HF-recovery	2.42 ± 0.68, b	136.10 ± 19.64	153.10 ± 15.83	6–7
$Lep^{+/+}$	1.43 ± 0.39	188.00 ± 37.11	154.30 ± 23.68	4–6
$Lep^{ob/ob}$	38.30 ± 15.25***, c	228.00 ± 52.26	158.60 ± 18.60	4–6
$Mc4R^{wt/wt}$	1.32 ± 0.52	169.30 ± 27.83	Not analyzed	6–8
$Mc4R^{X16/X16}$	7.22 ± 1.65***, a	147.30 ± 31.32	Not analyzed	6–8

Values are means ± SD. Data were analyzed by two-way ANOVA.
*$p < 0.05$, **$p < 0.01$, ***$p < 0.001$, significant differences compared to respective lean controls. Letters indicate significant group differences between obesity models.

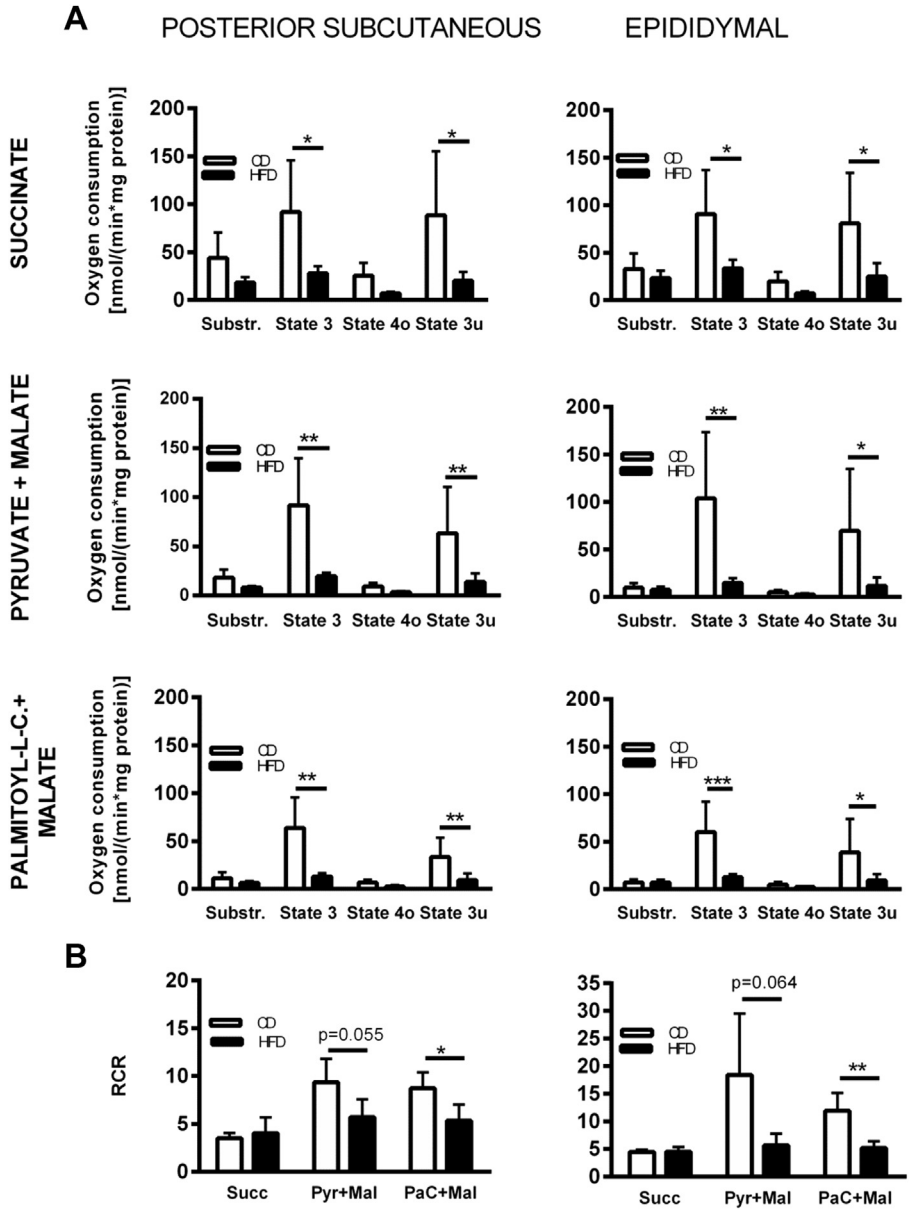

Figure 2: Bioenergetic characterization of isolated mitochondria from posterior subcutaneous and epididymal white adipocytes of mice fed either HFD or CD for 24 weeks: Obesity causes limited oxidative and respiratory capacity. (A) Bioenergetics of isolated white adipocyte mitochondria were measured using three different substrates (complex II linked substrate succinate and complex I linked substrates pyruvate or palmitate). First, respiration was assessed in presence of substrate only (state 4). Phosphorylating state 3 respiration was measured in the presence of ADP and substrate. ATP synthesis was inhibited and state 4o respiration was induced by oligomycin. Addition of the chemical uncoupler FCCP resulted in maximal uncoupled respiration (state 3u). Finally, non-biological background was determined by blockade of electron flow at complex III with antimycin A and subtracted from the other respiratory rates. Data were analyzed by Two-way repeated measures ANOVA (Bonferroni correction). (B) Mitochondrial respiratory control ratio (RCR) was calculated as indicator for mitochondrial integrity. It is defined as the ratio of state 3 to state 4o oxygen consumption (Succ = succinate, Pyr = pyruvate, Mal = malate, PaC = palmitoyl-L-carnitine). Data were analyzed by Student's t-test. Data are presented as means ± SD of 3–4 experiments.*$p = 0.05$, ** = $p < 0.01$, *** = $p < 0.001$.

released from the mitochondria or degraded by matrix antioxidant processes [22]. Mitochondrial H_2O_2 efflux, as a surrogate measure for ROS metabolism, was comparable in the two feeding groups of this study. We found no evidence for elevated ROS release from isolated white adipocyte mitochondria, which could be associated with impaired glucose tolerance observed in HFD fed mice. If anything, we detected a minor reduction of ROS release in mitochondria of the HFD group (Figure 4). This finding does not support the view that excessive mitochondrial ROS release in adipocytes from HFD fed mice contributes to the development of impaired glucose metabolism.

As oxygen consumption, but not ROS release, of isolated mitochondria was markedly affected in HFD fed mice, we further focused on respirometry. Studying intact cells prevents possible artifacts caused by the mitochondrial isolation procedure and is the most physiological approach to investigate cellular bioenergetics [4]. Therefore, we assessed whether the functional impairment observed in isolated mitochondria holds true for intact adipocytes. We observed no differences concerning basal and leak respiration but maximal cellular respiration rates in adipocytes (both fat depots) of the HFD group were markedly lower compared to the control group (Figure 5A,B).

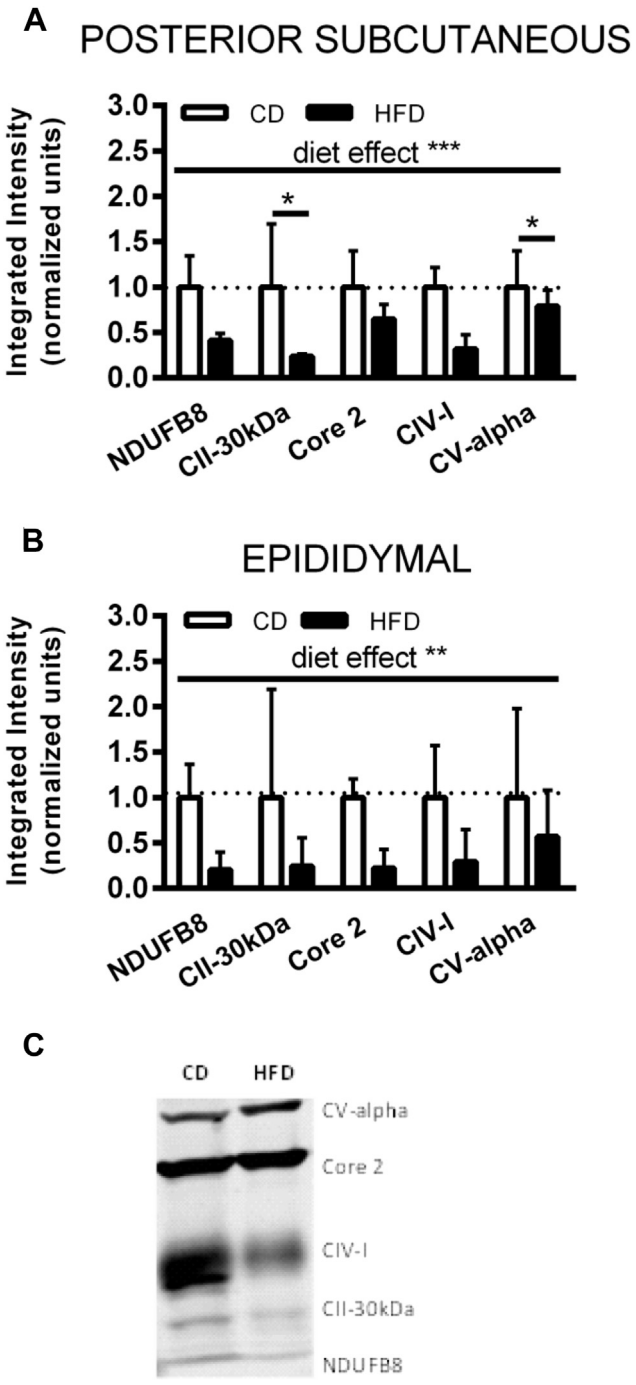

Figure 3: Reduced oxidative and respiratory capacity in white adipocyte mitochondria of HFD fed mice can be explained by lower enzymatic equipment of the respiratory chain. (A, B) Protein levels of representative subunits of each of the five OXPHOS complexes determined by immunoblot analysis of isolated mitochondria. MitoProfile® total OXPHOS antibody cocktail is targeted against complex I subunit NDUFB8, complex II-30kDa, complex III-Core protein 2, complex IV subunit I, and complex V alpha subunit. Bands were normalized to the outer membrane protein voltage-dependent anion channel (VDAC). Values of the HFD group are expressed as part of the CD group (=1). Data were analyzed by Two-way repeated measures ANOVA (Bonferroni correction) and presented as means ± SD of 3–4 experiments.*$p = 0.05$, ** $= p < 0.01$, *** $= p < 0.001$. (C) Representative OXPHOS immunoblot of isolated mitochondria from posterior subcutaneous adipocytes.

Accordingly, spare respiratory capacity — calculated as the difference in maximal and basal respiration — was lower in HFD adipocytes (Figure 5C,D). Thus, from a comparable basal level, adipocytes of HFD mice are unable to increase substrate oxidation in case of increased ATP demand to the same extent as adipocytes from control mice.

Differences in maximal respiratory capacity can be caused either by a different mitochondrial abundance per adipocyte, by a different functionality of mitochondria themselves, or by a combination of both. We quantified citrate synthase (CS) activity as a surrogate marker for mitochondrial abundance and observed lower mitochondrial mass in adipocytes of HFD fed versus CD fed mice, which only reached statistical significance for cells from posterior subcutaneous fat (Figure 5E,F). We calculated cell RCR (cRCR, maximal/leak respiration) as a measure for mitochondrial dysfunction, analogous to RCR of isolated mitochondria [4]. We observed reduced cRCRs for adipocytes of HFD fed mice in both fat depots analyzed but this reduction reached statistical significance only in epididymal fat (Figure 5G,H). Limited respiratory capacity in adipocytes of HFD fed mice can thus be explained by a combination of lower mitochondrial abundance per cell and insufficient mitochondrial OXPHOS capacity. The contribution of the latter is more prominent in adipocytes of epididymal fat.

We conclude that obesity caused by 24-weeks exposure to HFD results in glucose intolerance and a limitation in white adipocyte respiratory function. The latter is caused by both lower mitochondrial abundance per cell and impaired mitochondrial function as reflected by down-regulation of electron transport chain enzymes and reduced cRCRs/RCRs. Effects are more evident in adipocytes of epididymal as compared to posterior subcutaneous fat. We demonstrate simultaneous occurrence of reduced white adipocyte mitochondrial OXPHOS function and impaired glucose tolerance in the obese state.

3.2. Energy restriction rapidly recovers glucose tolerance, but not mitochondrial function

In a previous study, we found glucose tolerance of HFD fed mice to recover shortly after HFD is replaced by CD [23]. In detail, glucose tolerance of 12 weeks HFD fed mice of the strains AKR/J, SWR/J, and C57BL/6J was normalized after one week of CD refeeding. Of note, this phenomenon clearly occurred well in advance of a major decline in diet-induced body fat mass (unpublished data). This model should allow the dissection of a possible causality between white adipocyte mitochondrial function and glucose (in-)tolerance. Thus, we transferred the experimental design of our previous work to the present study and, in a second trial, refed mice with CD for one week after 24 weeks of HFD feeding (HF-recovery). During this period, HF-recovery mice markedly lost weight (HF-recovery -5.081 g $\pm$ 1.823 g vs. CD -0.064 g $\pm$ 1.640 g, $n = 7$, $p < 0.001$) but were still obese as indicated by final body weight and fat mass higher than that of controls (Figure 6A–B). Lean mass was comparable between the feeding groups (Figure 6C). Posterior subcutaneous and epididymal fat pads were significantly larger in HF-recovery compared to control mice, reflecting their contribution to whole body adiposity (posterior subcutaneous: HF-recovery 2.085 g $\pm$ 0.376 g vs. CD 0.732 g $\pm$ 0.280 g; epididymal: HF-recovery 1.540 g $\pm$ 0.156 g vs. CD 0.824 g $\pm$ 0.230 g, both $n = 7$, $p < 0.001$). Notably, HF-recovery mice displayed improved glucose tolerance which tended to be even better than that of controls (Figure 6D,E). To assess whether compensatory hyperinsulinemia masks peripheral insulin resistance, we analyzed plasma insulin levels. Compared to HFD fed mice HF-recovery mice stood out by significantly lower insulin concentrations which were similar to those of the control group (Table 1).

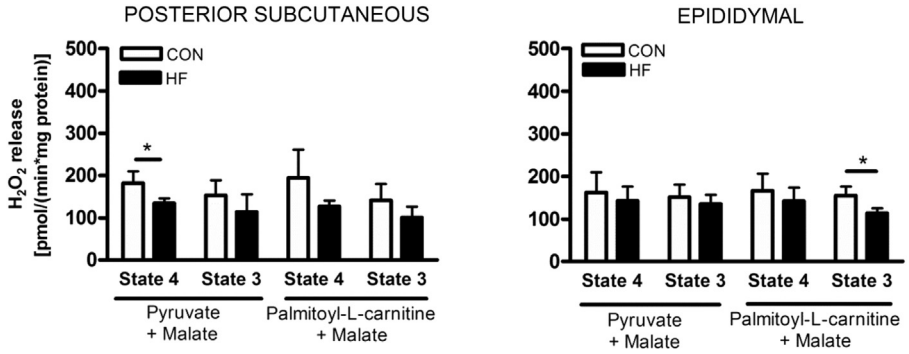

Figure 4: H_2O_2 release of isolated mitochondria from adipocytes of 24 weeks HFD versus CD fed mice. H_2O_2 release was assessed in pyruvate or palmitate energized mitochondria using Amplex® Red fluorescence. Measurements were conducted during state 4 (substrate only) and state 3 (substrate + ADP) respiration. Data are presented as means ± SD of 4 experiments. * = $p < 0.05$.

Respirometry of intact adipocytes revealed no difference between the CD und the HF-recovery group in basal and leak respiration. Maximal oxygen consumption of both types of adipocytes, however, was lower in the HF-recovery group (Figure 7A,B). Concordantly, spare respiratory capacity was reduced in adipocytes of HF-recovery mice (Figure 7C,D). Thus, adipocytes of HF-recovery mice displayed a lower ability to increase substrate oxidation compared to CD mice. Mitochondrial abundance, based on CS activity per cell, was reduced in adipocytes of HF-recovery mice (Figure 7E,F). Cellular RCR was comparable in posterior subcutaneous but markedly decreased in epididymal adipocytes (Figure 7G,H). Thus, limited maximal cellular respiration in epididymal adipocytes is clearly ascribable to both lower mitochondrial

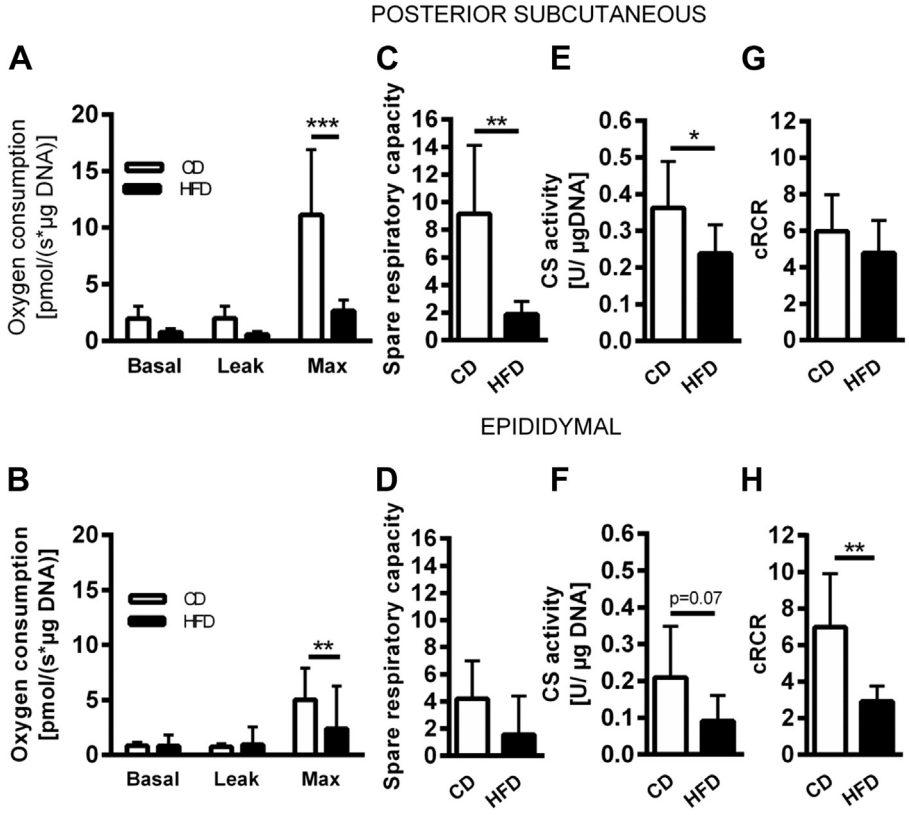

Figure 5: Cellular respiration of adipocytes from mice either fed HFD or CD for 24 weeks: HFD feeding results in limited maximal cellular respiratory capacity and reduced mitochondrial integrity. (A, B) First, basal respiration using pyruvate as substrate was assessed. ATP synthase inhibitor oligomycin was added to define the proportion of basal respiration contributing to either ATP turnover or proton leak, respectively. Next, FCCP was added to determine the maximal cellular respiratory capacity. Lastly, non-mitochondrial background was determined by addition of complex III inhibitor antimycin A and subtracted from the other respiratory states. Oxygen consumption rates are expressed per µg DNA. (C, D) Higher spare respiratory capacity in adipocytes from CD fed mice. Spare respiratory capacity = max − basal. (E, F) Citrate synthase activity was measured as a marker for mitochondrial abundance and expressed as CS activity per µg DNA (G, H). As an index for mitochondrial integrity, cell respiratory control ratio (cRCR) was calculated (quotient of maximal to leak oxygen consumption). A–B was analyzed by Two-way repeated measures ANOVA (Bonferroni correction. C-H was analyzed by Student's t-test. Data are presented as means ± SD of 7 experiments. $p < 0.05$, ** = $p < 0.01$, *** = $p < 0.001$.

abundance and lower mitochondrial capacity. In posterior subcutaneous adipocytes, mitochondrial abundance alone explains the diminished cellular respiratory capacity.

Taken together, obese HF-recovery mice exhibited limited mitochondrial OXPHOS capacity in white adipocytes, with stronger effects in epididymal vs. subcutaneous fat, i.e. in a similar pattern as observed in adipocytes of obese HFD fed mice. Notably, these mice displayed a normal, undisturbed glucose tolerance. As euglycemia was maintained by normal insulin levels, pancreatic overcompensation as a reason for normalized glucose tolerance is highly unlikely. In this model, we thus observed a clear dissociation of reduced white adipocyte mitochondrial OXPHOS capacity from impaired glucose tolerance.

3.3. Monogenetic models of obesity: different glucose tolerance but similar white adipocyte mitochondrial OXPHOS capacity

In a mouse model of diet induced obesity we observed an association between white adipocyte mitochondrial function and glucose tolerance in the obese state but a dissociation during remission. To rule out direct effects of diet or catabolism, we extended our study to monogenetic models of obesity. $Lep^{ob/ob}$ mice and mice with melanocortin-4-receptor (Mc4R) deficiency, including $Mc4R^{X16/X16}$, are well established models of monogenetic obesity characterized by enormous weight and fat mass gain on a regular diet [15,16].

Mutant mice of both models were heavily obese (Figure 8A,B; Table 2). Accordingly, posterior subcutaneous and epididymal fat pads were larger compared to wildtype mice (Table 2). Oral glucose tolerance tests revealed impaired glucose tolerance in $Lep^{ob/ob}$ mice as indicated by lower glucose clearance and higher total AUC (Figure 8A). In contrast, oral glucose tolerance of $Mc4R^{X16/X16}$ and $Mc4R^{wt/wt}$ mice was comparable (Figure 8B). At the same time, plasma insulin of $Lep^{ob/ob}$ was more than 5 times higher than plasma insulin of $Mc4R^{X16/X16}$ mice, indicating better peripheral insulin sensitivity rather than pancreatic compensation as a reason for normalized glucose tolerance in the $Mc4R^{X16/X16}$ mice (Table 1). Notably, mitochondrial OXPHOS capacity of both mutants, reflected by cRCR, tended to be lower in posterior subcutaneous adipocytes and was massively decreased in epididymal adipocytes (Figure 8A,B).

In summary, we observed simultaneous occurrence of impaired glucose tolerance and white adipocyte mitochondrial OXPHOS function in $Lep^{ob/ob}$ mice. $Mc4R^{X16/X16}$ mice, however, showed impaired OXPHOS capacity paralleled by normal glucose tolerance.

Reduced white adipocyte OXPHOS capacity seems to be a hallmark of obesity, especially in adipocytes of intraabdominal origin. It is not, however, necessarily accompanied by whole body glucose intolerance. This conclusion holds true for both the catabolic state (HF-recovery mice) and the anabolic state ($Mc4R^{X16/X16}$).

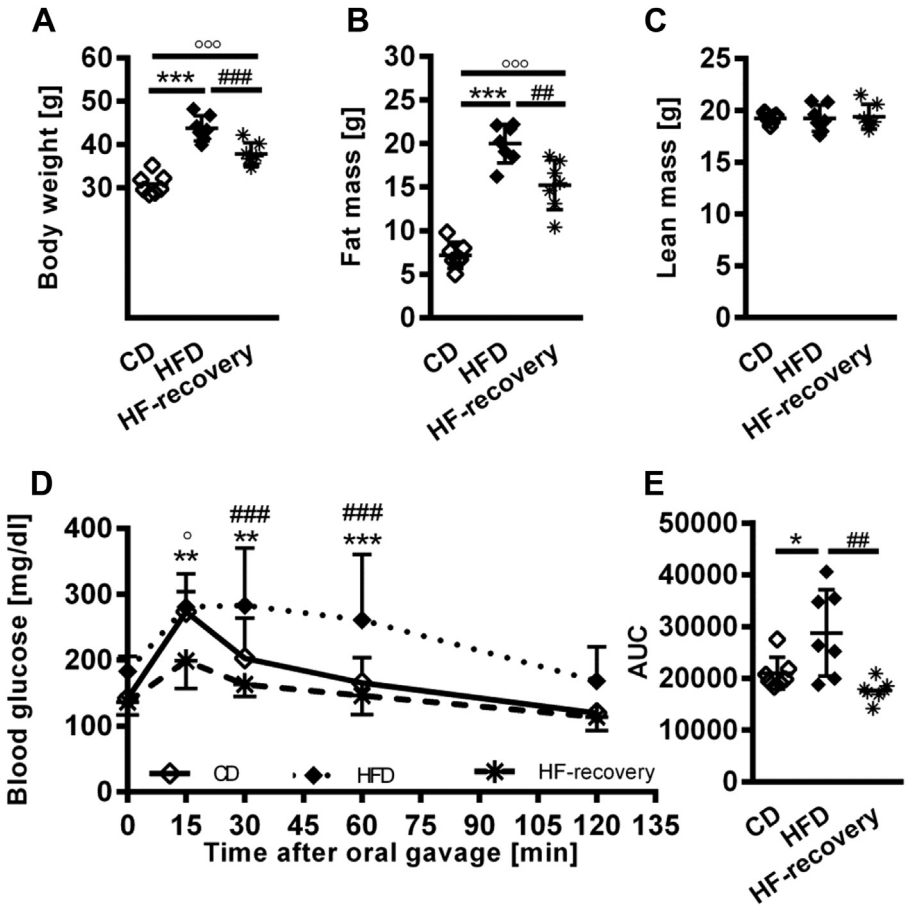

Figure 6: One week refeeding CD following 24 weeks HFD (HF-recovery) is sufficient to restore glucose tolerance. At the age of eight weeks, mice were matched by body weight into HFD and CD groups. The respective diet was fed for 24 weeks then HFD fed mice received CD for one week. (A) Body weight, (B) Fat mass, (C) Lean mass, (D) Oral glucose tolerance test, (E) Total area-under-the-curve (AUC) calculated from D as measure for glucose tolerance. Values of the HF-recovery group are shown both before and after one week CD refeeding. A-E were analyzed by one-way ANOVA. D was analyzed by two way repeated measures ANOVA, * corresponds to comparison between CD and HFD, ° corresponds to comparison between CD and HF-recovery, # corresponds to comparison between HFD and HF-recovery, n = 7, */#/° = $p < 0.05$, **/##/°° = $p < 0.01$, ***/###/°°° = $p < 0.001$.

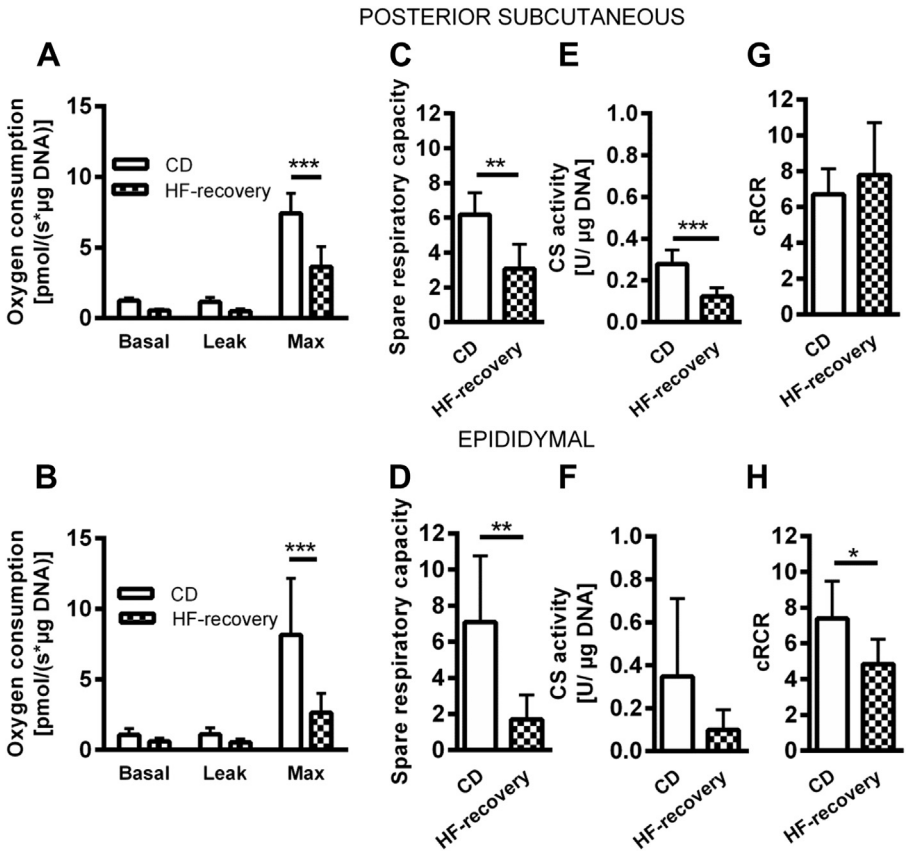

Figure 7: Cellular respiration of adipocytes from HF-recovery and CD mice. Recovery intervention does not restore limited maximal respiratory capacity and reduced mitochondrial integrity. (A, B) First, basal respiration was assessed using pyruvate as a substrate. ATP synthase inhibitor oligomycin was added to define the proportion of basal respiration contributing to either ATP turnover or proton leak, respectively. Next, FCCP was added to determine the maximal cellular respiratory capacity. Lastly, non-mitochondrial background was determined by addition of complex III inhibitor antimycin A and subtracted from the other respiratory states. Oxygen consumption rates are expressed per µg DNA. (C, D) Spare respiratory capacity = max − basal. (E, F) Citrate synthase activity was measured as marker for mitochondrial abundance and expressed as CS activity per µg DNA. (G, H) Cell respiratory control ratio (cRCR) was calculated as an index for mitochondrial integrity (quotient of maximal to leak oxygen consumption). A-B was analyzed by Two-way repeated measures ANOVA (Bonferroni correction. C-H was analyzed by Student's t-test. Data are presented as means ± SD of 5–7 experiments. $p < 0.05$, ** = $p < 0.01$, *** = $p < 0.001$.

4. DISCUSSION

It has been repeatedly proposed that altered mitochondrial metabolism of adipocytes in WAT plays a key role in the development of obesity associated impaired glucose homeostasis [14,24–27]. Clarifying the relation between white adipocyte mitochondrial alterations and impaired glucose homeostasis in obesity is thus of enormous interest. The goal of the present study was to elucidate whether alterations in white adipocyte mitochondrial respiratory function are a phenomenon of obesity, of impaired glucose tolerance, or of both, with the latter allowing further speculations about a potential causal link. We phenotyped four common murine obesity models for the status of glucose tolerance and white adipocyte mitochondrial oxidative phosphorylation (OXPHOS) function in subcutaneous as well as intraabdominal fat.

In all our model systems, obesity was generally associated with reduced white adipocyte mitochondrial OXPHOS capacity as detected by decreased cell respiratory control ratio (cRCR) in adipocytes of obese mice, particularly in cells of intraabdominal origin. As a ratio of maximal to leak respiration, cRCR is both sensitive to changes in maximal substrate oxidation capacity and proton leak [4]. The low cRCRs found in adipocytes of obese mice can thus be caused by either high proton leak, low maximal substrate oxidation capacity, or a combination of both. In this study, limitations in cRCR of adipocyte mitochondria from obese mice were mainly caused by diminished maximal substrate oxidation capacity and not by increased proton leak (Figure S1). Strikingly, impaired OXPHOS capacity was not necessarily accompanied by impaired whole body glucose tolerance. HF-recovery and $Mc4R^{X16/X16}$ mice where characterized by normal glucose tolerance despite impaired mitochondrial OXPHOS capacity, mainly in epididymal white adipocytes. Of note, normalized glucose tolerance seemed not to be caused by pancreatic overcompensation but rather by improved peripheral insulin sensitivity as plasma insulin levels appeared quite low.

We conclude that glucose intolerance occurs independently of OXPHOS impairment in white adipocytes, thus excluding the latter as a proximate trigger for impaired glucose homeostasis in obesity. Alternatively, in a scenario of complex systemic regulation, additional permissive factors unknown so far may link reduced white adipocyte mitochondrial OXPHOS to impaired glucose metabolism. In other words, impaired respiratory capacity in white adipocytes solely is not sufficient for the development of systemic glucose intolerance.

Mechanistically, reduced OXPHOS could represent an adaptive mechanism to energy overload, adipocyte hypertrophy, and massive adipose tissue expansion. First, there is evidence for relative hypoxia in

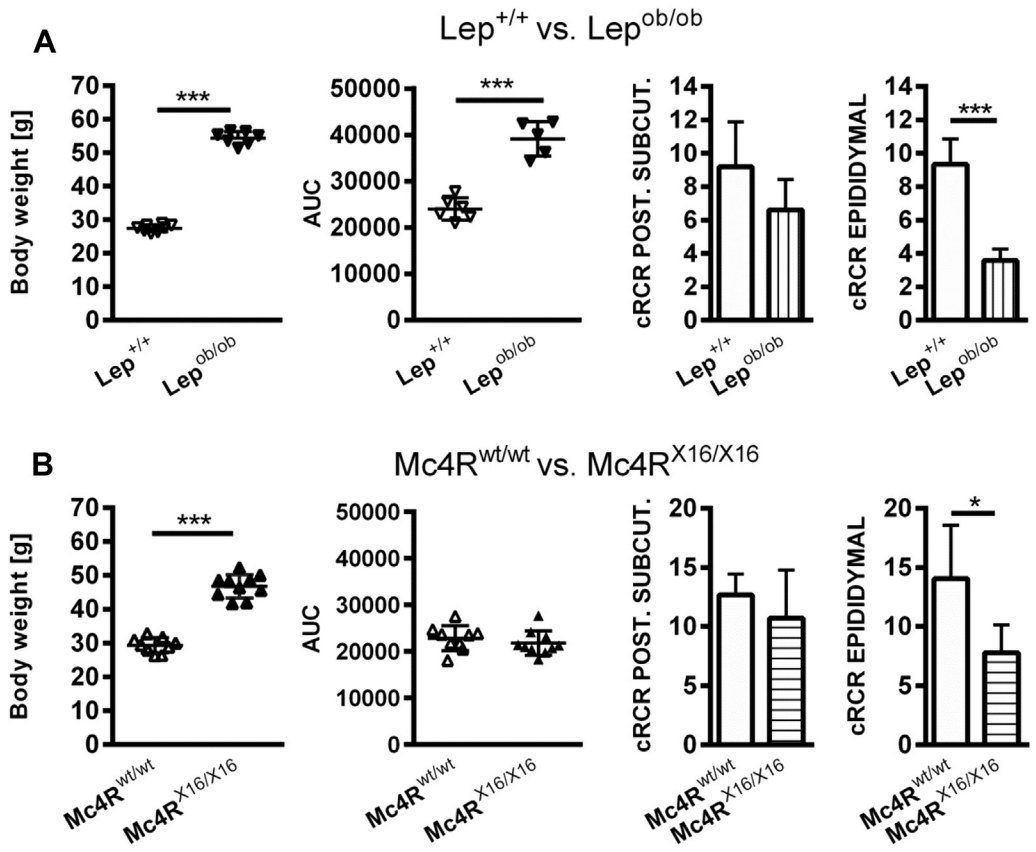

Figure 8: Monogenetic models of obesity: Differences in glucose tolerance but similarities in white adipocyte mitochondrial OXPHOS capacity. (A) **Comparison of Lep$^{ob/ob}$ mice and Lep$^{+/+}$ littermates**. Lep$^{ob/ob}$ mice show massive obesity and impaired glucose tolerance measured by total area-under-the-curve (AUC) ($n = 5–8$). (B) **Comparison of Mc4R$^{X16/X16}$ and Mc4R$^{wt/wt}$ littermates**. Mc4R$^{X16/X16}$ mice show massive obesity but normal glucose tolerance measured by total area-under-the-curve (AUC) ($n = 5–9$). (A) and (B) Mitochondrial integrity in epididymal white adipocytes is affected in both models as indicated by lowered cell respiratory capacity (cRCR). All data were analyzed by Student's t-test. Bars are presented as means ± SD. $p < 0.05$, *** = $p < 0.001$.

WAT of obese rodents. In Lep$^{ob/ob}$ and diet-induced obese mice, oxygen partial pressure is reduced 2- to 3-fold in WAT compared to lean controls [28,29]. In hypoxic WAT there may be no need for a high mitochondrial capacity since adipocytes switch from aerobic OXPHOS to anaerobic glycolysis to compensate for diminished aerobic oxidation [30–34]. Consequently, this could trigger a reduction of mitochondrial power determined by loss of mitochondrial mass, substrate oxidation capacity of the electron transport chain, and coupling efficiency. Reduced OXPHOS capacity, however, does not necessarily result in ATP-depletion, energetic stress, or adipocyte dysfunction; cellular ATP homeostasis obviously can be maintained by glycolytic ATP production as transgenic manipulation of adipocyte mitochondria and subsequent OXPHOS impairment does not change ATP levels in WAT [24].

Table 2 – Body composition and fat pad weights of Lep$^{+/+}$ vs. Lep$^{ob/ob}$ and Mc4R$^{wt/wt}$ vs. Mc4R$^{X16/X16}$ mice.

Lep$^{+/+}$ vs. Lep$^{ob/ob}$			
	Lep$^{+/+}$	Lep$^{ob/ob}$	n
Fat mass [g]	3.50 ± 0.61	32.80 ± 1.61***	5
Lean mass [g]	19.61 ± 0.40	16.28 ± 0.70***	5
psWAT mass [mg]	275.3 ± 63.5	2828 ± 388.7***	7–8
eWAT mass [mg]	339.1 ± 83.1	3571 ± 182.6***	7–8
Mc4R$^{wt/wt}$ vs. Mc4R$^{X16/X16}$			
	Mc4R$^{wt/wt}$	Mc4R$^{X16/X16}$	n
Fat mass [g]	4.26 ± 1.20	18.78 ± 3.02***	9–10
Lean mass [g]	20.84 ± 1.11	23.02 ± 0.94***	9–10
psWAT mass [mg]	432.8 ± 112.8	2421 ± 315.4***	9
eWAT mass [mg]	435.5 ± 170.5	2103 ± 465.9***	9

Values are means ± SD. Data were analyzed by Student's t-test.
*** = $p < 0.001$, significant differences compared to respective lean controls (Lep$^{+/+}$ or Mc4R$^{wt/wt}$).

Second, studies in mice, rats, and humans revealed downregulation of *de novo* lipogenesis in adipose tissue in obesity [35–37], which has been suggested as an adaptive process to limit an ongoing increase of fat mass [37]. Cellular ATP demand for lipogenic enzyme activity, and the resulting requirement for mitochondrial OXPHOS activity for this process, would therefore be reduced. Accordingly, expression of acetyl-CoA carboxylase, the rate-limiting lipogenic enzyme catalyzing the ATP-dependent first step of fatty acid synthesis, is reduced in obesity [36,37]. Of note, hypoxia inhibits lipogenesis and may thus act synergistically in this context [38]. In our study, decreased white adipocyte mitochondrial abundance and respiratory capacity were always accompanied by a body energy surplus and increased fat pad weight. It is therefore plausible that reduced mitochondrial OXPHOS capacity represents an adaptive, non-pathological mechanism of adipocytes coping with hypoxia in WAT and/or reduced cellular ATP demand.

Impaired mitochondria have earlier been observed in obesity and/or states of altered glucose homeostasis [8–13,39]. Very recently, network-based integration of enriched biological processes, respective regulators and related physiological changes revealed changes of

mitochondrial function in murine epididymal fat that notably continuously deteriorate during prolonged HF-diet feeding [40]. To date, however, these alterations have not been studied in detail on the functional level, i.e. by precise respirometry of both mitochondria and cells in differently energized states and with different substrates. Thus, we here comprehensively analyzed mitochondrial OXPHOS of obese and glucose intolerant versus lean and healthy mice applying state-of-the-art respirometry technologies and additional biochemical techniques. OXPHOS capacity in both adipocytes of 24-weeks high-fat diet (HFD) fed mice and their isolated mitochondria were reduced in states where maximal substrate oxidation capacity determines oxygen consumption (state 3, state 3u, max). On the level of isolated mitochondria this can be explained by limited enzymatic equipment of the respiratory chain. On the cellular level, this deficit is amplified by reduced white adipocyte mitochondrial abundance. Importantly, integrity of mitochondria from adipocytes of both fat depots, indicated by RCRs, is affected when mitochondria are energized with complex I (pyruvate, palmitate) but not complex II (succinate) linked substrates. Thus, our comprehensive analysis on isolated white adipocyte mitochondria of HFD vs. CD fed mice revealed differences in RCR depending on electron entry site into the respiratory chain. The molecular mechanisms determining this difference have to be addressed in future studies.

In summary, we analyzed the impact of obesity on white adipocyte mitochondrial respiratory function in anatomically distinct fat depots and whole body glucose metabolism with a focus on a possible association between both phenomena. We utilized four models of diet-induced or genetic obesity characterized by either impaired or normal oral glucose tolerance. We identified reduced mitochondrial OXPHOS in white adipocytes to be a general hallmark of obesity, but to be independent of glucose tolerance status.

DISCLOSURE

The authors have nothing to disclose.

ACKNOWLEDGMENTS

The Chair of Molecular Nutritional Medicine received financial support from the Else Kröner-Fresenius Foundation (2007–2014). This study was partly funded by the Federal Ministry of Education and Research, Germany (BMBF AZ 0315674) and was supported by the Technische Universität München within the funding program Open Access Publishing.

CONFLICT OF INTEREST

None declared.

APPENDIX A. SUPPLEMENTARY DATA

Supplementary data related to this article can be found at http://dx.doi.org/10.1016/j.molmet.2015.07.001.

REFERENCES

[1] Elia, M., 1992. Organ and tissue contribution to metabolic rate. In: Kinney, J., Tucker, H. (Eds.), Energy metabolism: tissue determinants and cellular corollaries. New York: Raven Press. p. 61–80.

[2] Wang, Z., Ying, Z., Bosy-Westphal, A., Zhang, J., Schautz, B., Later, W., et al., 2010. Specific metabolic rates of major organs and tissues across adulthood: evaluation by mechanistic model of resting energy expenditure. American Journal of Clinical Nutrition 92(6):1369–1377.

[3] Kaiyala, K.J., Morton, G.J., Leroux, B.G., Ogimoto, K., Wisse, B., Schwartz, M.W., 2010. Identification of body fat mass as a major determinant of metabolic rate in mice. Diabetes 59(7):1657–1666.

[4] Brand, M.D., Nicholls, D.G., 2011. Assessing mitochondrial dysfunction in cells. Biochemical Journal 435(2):297–312.

[5] Stehling, O., Wilbrecht, C., Lill, R., 2014. Mitochondrial iron-sulfur protein biogenesis and human disease. Biochimie 100:61–77.

[6] De Pauw, A., Tejerina, S., Raes, M., Keijer, J., Arnould, T., 2009. Mitochondrial (dys)function in adipocyte (de)differentiation and systemic metabolic alterations. American Journal of Pathology 175(3):927–939.

[7] Koh, E.H., Park, J.Y., Park, H.S., Jeon, M.J., Ryu, J.W., Kim, M., et al., 2007. Essential role of mitochondrial function in adiponectin synthesis in adipocytes. Diabetes 56(12):2973–2981.

[8] Hallgren, P., Sjostrom, L., Hedlund, H., Lundell, L., Olbe, L., 1989. Influence of age, fat cell weight, and obesity on O_2 consumption of human adipose tissue. American Journal of Physiology 256(4 Pt 1):E467–E474.

[9] Choo, H.J., Kim, J.H., Kwon, O.B., Lee, C.S., Mun, J.Y., Han, S.S., et al., 2006. Mitochondria are impaired in the adipocytes of type 2 diabetic mice. Diabetologia 49(4):784–791.

[10] Rong, J.X., Qiu, Y., Hansen, M.K., Zhu, L., Zhang, V., Xie, M., et al., 2007. Adipose mitochondrial biogenesis is suppressed in db/db and high-fat diet-fed mice and improved by rosiglitazone. Diabetes 56(7):1751–1760.

[11] Valerio, A., Cardile, A., Cozzi, V., Bracale, R., Tedesco, L., Pisconti, A., et al., 2006. TNF-alpha downregulates eNOS expression and mitochondrial biogenesis in fat and muscle of obese rodents. Journal of Clinical Investigation 116(10):2791–2798.

[12] Wilson-Fritch, L., Nicoloro, S., Chouinard, M., Lazar, M.A., Chui, P.C., Leszyk, J., et al., 2004. Mitochondrial remodeling in adipose tissue associated with obesity and treatment with rosiglitazone. Journal of Clinical Investigation 114(9):1281–1289.

[13] Dahlman, I., Forsgren, M., Sjogren, A., Nordstrom, E.A., Kaaman, M., Naslund, E., et al., 2006. Downregulation of electron transport chain genes in visceral adipose tissue in type 2 diabetes independent of obesity and possibly involving tumor necrosis factor-alpha. Diabetes 55(6):1792–1799.

[14] Schottl, T., Kappler, L., Braun, K., Fromme, T., Klingenspor, M., 2014. Limited mitochondrial capacity of visceral versus subcutaneous white adipocytes in male C57BL/6N mice. Endocrinology en20141689.

[15] Fellmann, L., Nascimento, A.R., Tibirica, E., Bousquet, P., 2013. Murine models for pharmacological studies of the metabolic syndrome. Pharmacology & Therapeutics 137(3):331–340.

[16] Bolze, F., Rink, N., Brumm, H., Kuhn, R., Mocek, S., Schwarz, A.E., et al., 2013. Characterization of the melanocortin-4-receptor nonsense mutation W16X in vitro and in vivo. Pharmacogenomics Journal 13(1):80–93.

[17] Even, P.C., Nadkarni, N.A., 2012. Indirect calorimetry in laboratory mice and rats: principles, practical considerations, interpretation and perspectives. American Journal of Physiology. Regulatory, Integrative and Comparative Physiology 303(5):R459–R476.

[18] Boudina, S., Sena, S., O'Neill, B.T., Tathireddy, P., Young, M.E., Abel, E.D., 2005. Reduced mitochondrial oxidative capacity and increased mitochondrial uncoupling impair myocardial energetics in obesity. Circulation 112(17):2686–2695.

[19] Wang, P.W., Kuo, H.M., Huang, H.T., Chang, A.Y., Weng, S.W., Tai, M.H., et al., 2014. Biphasic response of mitochondrial biogenesis to oxidative stress in visceral fat of diet-induced obesity mice. Antioxidants & Redox Signaling.

[20] Loschen, G., Azzi, A., Richter, C., Flohe, L., 1974. Superoxide radicals as precursors of mitochondrial hydrogen peroxide. FEBS Letters 42(1):68–72.

[21] Loschen, G., Azzi, A., 1975. On the formation of hydrogen peroxide and oxygen radicals in heart mitochondria. Recent Advances in Studies on Cardiac Structure and Metabolism 7:3–12.

[22] Treberg, J.R., Quinlan, C.L., Brand, M.D., 2010. Hydrogen peroxide efflux from muscle mitochondria underestimates matrix superoxide production — a correction using glutathione depletion. FEBS Journal 277(13):2766—2778.
[23] Kless, C., Klingenspor, M., 2013. Metabolic status of adipocytes triggers rapid adjustments of systemic glucose tolerance. FASEB Journal 27 (1071.2).
[24] Ryu, M.J., Kim, S.J., Kim, Y.K., Choi, M.J., Tadi, S., Lee, M.H., et al., 2013. Crif1 deficiency reduces adipose OXPHOS capacity and triggers inflammation and insulin resistance in mice. PLoS Genetics 9(3):e1003356.
[25] Keuper, M., Jastroch, M., Yi, C.X., Fischer-Posovszky, P., Wabitsch, M., Tschop, M.H., et al., 2014. Spare mitochondrial respiratory capacity permits human adipocytes to maintain ATP homeostasis under hypoglycemic conditions. FASEB Journal 28(2):761—770.
[26] Kusminski, C.M., Scherer, P.E., 2012. Mitochondrial dysfunction in white adipose tissue. Trends in Endocrinology Metabolism 23(9):435—443.
[27] Lee, Y.S., Kim, J.W., Osborne, O., Oh da, Y., Sasik, R., Schenk, S., et al., 2014. Increased adipocyte O_2 consumption triggers HIF-1alpha, causing inflammation and insulin resistance in obesity. Cell 157(6):1339—1352.
[28] Ye, J., Gao, Z., Yin, J., He, Q., 2007. Hypoxia is a potential risk factor for chronic inflammation and adiponectin reduction in adipose tissue of ob/ob and dietary obese mice. American Journal of Physiology, Endocrinology and Metabolism 293(4):E1118—E1128.
[29] Rausch, M.E., Weisberg, S., Vardhana, P., Tortoriello, D.V., 2008. Obesity in C57BL/6J mice is characterized by adipose tissue hypoxia and cytotoxic T-cell infiltration. International Journal of Obesity (London) 32(3):451—463.
[30] Choi, S., Cho, K., Kim, J., Yea, K., Park, G., Lee, J., et al., 2009. Comparative proteome analysis using amine-reactive isobaric tagging reagents coupled with 2D LC/MS/MS in 3T3-L1 adipocytes following hypoxia or normoxia. Biochemical and Biophysical Research Communications 383(1):135—140.
[31] Perez de Heredia, F., Wood, I.S., Trayhurn, P., 2010. Hypoxia stimulates lactate release and modulates monocarboxylate transporter (MCT1, MCT2, and MCT4) expression in human adipocytes. Pflugers Archiv 459(3):509—518.
[32] Wood, I.S., Wang, B., Lorente-Cebrian, S., Trayhurn, P., 2007. Hypoxia increases expression of selective facilitative glucose transporters (GLUT) and 2-deoxy-D-glucose uptake in human adipocytes. Biochemical and Biophysical Research Communications 361(2):468—473.
[33] Trayhurn, P., Alomar, S.Y., 2015. Oxygen deprivation and the cellular response to hypoxia in adipocytes — perspectives on white and brown adipose tissues in obesity. Frontiers in Endocrinology (Lausanne) 6:19.
[34] Geiger, K., Leiherer, A., Muendlein, A., Stark, N., Geller-Rhomberg, S., Saely, C.H., et al., 2011. Identification of hypoxia-induced genes in human SGBS adipocytes by microarray analysis. PLoS One 6(10):e26465.
[35] Diraison, F., Dusserre, E., Vidal, H., Sothier, M., Beylot, M., 2002. Increased hepatic lipogenesis but decreased expression of lipogenic gene in adipose tissue in human obesity. American Journal of Physiology, Endocrinology Metabolism 282(1):E46—E51.
[36] Vida, M., Rivera, P., Gavito, A.L., Suarez, J., Pavon, F.J., Arrabal, S., et al., 2014. CB1 blockade potentiates down-regulation of lipogenic gene expression in perirenal adipose tissue in high carbohydrate diet-induced obesity. PLoS One 9(2):e90016.
[37] Ortega, F.J., Mayas, D., Moreno-Navarrete, J.M., Catalan, V., Gomez-Ambrosi, J., Esteve, E., et al., 2010. The gene expression of the main lipogenic enzymes is downregulated in visceral adipose tissue of obese subjects. Obesity (Silver Spring) 18(1):13—20.
[38] O'Rourke, R.W., Meyer, K.A., Gaston, G., White, A.E., Lumeng, C.N., Marks, D.L., 2013. Hexosamine biosynthesis is a possible mechanism underlying hypoxia's effects on lipid metabolism in human adipocytes. PLoS One 8(8):e71165.
[39] Yin, X., Lanza, I.R., Swain, J.M., Sarr, M.G., Nair, K.S., Jensen, M.D., 2013. Adipocyte mitochondrial function is reduced in human obesity independent of fat cell size. Journal of Clinical Endocrinology and Metabolism jc20133042.
[40] Derous, D., Kelder, T., van Schothorst, E.M., van Erk, M., Voigt, A., Klaus, S., et al., 2015. Network-based integration of molecular and physiological data elucidates regulatory mechanisms underlying adaptation to high-fat diet. Genes Nutrition 10(4):470.

